Strength of Correlation Effects in the Electronic Structure of Iron

J. Sánchez-Barriga,[1] J. Fink,[1,2] V. Boni,[3] I. Di Marco,[4,5] J. Braun,[6] J. Minár,[6] A. Varykhalov,[1] O. Rader,[1] V. Bellini,[3] F. Manghi,[3] H. Ebert,[6] M. I. Katsnelson,[5] A. I. Lichtenstein,[7] O. Eriksson,[4] W. Eberhardt,[1] and H. A. Dürr[1]

[1]*Helmholtz-Zentrum Berlin für Materialien und Energie, Elektronenspeicherring BESSY II, Albert-Einstein-Strasse 15, D-12489 Berlin, Germany*

[2]*Leibniz-Institute for Solid State and Materials Research Dresden, Post Office Box 270116, D-01171 Dresden, Germany*

[3]*Dipartimento di Fisica, Università di Modena, Via Campi 213/a, I-41100 Modena, Italy*

[4]*Department of Physics and Material Science, Uppsala University, Box 530, SE-751 21 Uppsala, Sweden*

[5]*Institute of Molecules and Materials, Radboud University of Nijmegen, Heijendaalsweg 135, 6525 AJ Nijmegen, The Netherlands*

[6]*Dep. Chemie und Biochemie, Physikalische Chemie, Universität München, Butenandtstr. 5-13, D-81377 München, Germany*

[7]*Institute of Theoretical Physics, University of Hamburg, 20355 Hamburg, Germany*

(Received 16 October 2009; published 23 December 2009)

The strength of electronic correlation effects in the spin-dependent electronic structure of ferromagnetic bcc Fe(110) has been investigated by means of spin and angle-resolved photoemission spectroscopy. The experimental results are compared to theoretical calculations within the three-body scattering approximation and within the dynamical mean-field theory, together with one-step model calculations of the photoemission process. This comparison indicates that the present state of the art many-body calculations, although improving the description of correlation effects in Fe, give too small mass renormalizations and scattering rates thus demanding more refined many-body theories including nonlocal fluctuations.

DOI: 10.1103/PhysRevLett.103.267203 PACS numbers: 75.70.Rf, 71.15.Mb, 73.20.At, 79.60.Bm

For more than half a century, it has been clear that the band structure together with exchange and correlation effects play an important role in the appearance of ferromagnetism in 3*d* transition metals and their alloys [1]. A first step toward an understanding of the electronic structure of these metals has been achieved by calculations of the single-particle band dispersion [$E(\mathbf{k})$] within the density functional theory (DFT) in the local spin-density approximation (LSDA) [2], which takes into account correlation effects only in a limited extent. It soon turned out that for the ferromagnetic 3*d* transition metals such as Fe, Co, and Ni, calculations beyond DFT-based theories have to be developed to take into account many-body interaction, i.e., correlation effects, which normally are described by the energy and momentum dependent complex self-energy function $\Sigma(E, \mathbf{k})$. Here, the real part $\Re\Sigma$ is related to the mass enhancement while the imaginary part $\Im\Sigma$ describes the scattering rate. One of the successful schemes for correlated electron systems is the dynamical mean-field theory (DMFT). It replaces the problem of describing correlation effects in a periodic lattice by a correlated impurity coupled to a self-consistent bath [3]. An alternative approach is the three-body scattering (3BS) approximation which takes into account the scattering of a hole into an Auger-like excitation in the valence band, formed by one hole plus an electron-hole excitation [4]. Such many-body calculations allowed the qualitative description of the quenching of majority-channel quasiparticle excitations in Co [5] or the narrowing of the Ni 3*d* band [6]. While the above-mentioned many-body theories give an improved description of the electronic structure, the central question is whether they also lead to a *quantitative* agreement with experiments.

Angle-resolved photoemission spectroscopy (ARPES) is a powerful method to determine the spectral function and by comparison with the bare-particle band structure (usually approximated by DFT band structure calculations) to obtain the self-energy [7]. Moreover, the spin-resolved version of this method is very useful to disentangle the complex electronic structure of ferromagnets, in particular, for systems with a strong overlap between majority and minority bands [8]. For ferromagnetic bcc Fe, which is the focus of the present work, several (spin-resolved) ARPES studies have been presented in the literature [9–13].

In this Letter, we present (spin-resolved) ARPES spectra of ferromagnetic bcc Fe(110). These experimental results are compared to theoretical many-body calculations (DMFT and 3BS) as mentioned above, including a full calculation of the one-step photoemission process. Our main conclusion is that a quantitative agreement, in particular, concerning the line widths, is not observed. This clearly demonstrates the demand for further nonlocal many-body theories.

Experiments have been performed at room temperature in normal emission using a hemispherical SPECS Phoibos 150 electron energy analyzer and undulator radiation from the UE112-PGM1 beam line at BESSY II. The linear polarization of the photon beam could be switched from horizontal to vertical, which means that a more $p-(\mathbf{A}||[1\bar{1}0])$ or $s-(\mathbf{A}||[001])$ character of the incident light was achieved, respectively. For spin analysis, a Rice University Mott-type spin polarimeter has been used, operated at 26 kV [14]. The angular resolution of the equip-

ment was 1°, and the energy resolution was 100 meV. The Fe(110) surface has been prepared on W(110) by deposition of 20 ML Fe and post-annealing. The structural quality of the films has been checked by low-energy electron diffraction. The Fe(110) film was remanently magnetized in the film plane along the $[1\bar{1}0]$ easy axis.

Theoretical calculations of the ARPES spectra have been performed within the framework of the Korringa-Kohn-Rostoker multiple scattering theory [15]. Spin-orbit coupling and exchange splitting were treated on equal footing in a fully relativistic theory. To account for electronic correlations beyond the LSDA approximation, a site-diagonal, local and complex energy-dependent self-energy Σ_{DMFT} was introduced self-consistently [16]. In most of the calculations presented for the comparison with the ARPES results, unless specified, we use for the averaged on-site Coulomb interaction U a value $U = 1.5$ eV which is within the experimental value $U \approx 1$ eV [17] and a value $U \approx 2$ eV derived from theoretical studies [18,19]. It is usually accepted that the averaged on-site exchange interaction J coincides with its atomic value $J \sim 0.9$ eV [20]. Using this LSDA + DMFT approach, the spectral function $A(E, \mathbf{k})$ could be calculated for a semi-infinite lattice structure. For a quantitative comparison with the measured ARPES spectra, it is inevitable to take into account the wave-vector and energy-dependent transition matrix elements calculated within the one-step model of photoemission (1SM) [21]. This describes the excitation process, the transport of the photoelectrons to the surface, as well as the escape into the vacuum. For a quantitative description of surface states and resonances, a realistic approach for the surface barrier is essential. Finally, analogous calculations of the ARPES signal have been performed on the basis of the 3BS self-energy function. The two calculations (3BS and DMFT) do not show big differences. We emphasize that in all the calculations, the broadening of the peaks due to final state effects is included.

Figures 1(a) and 1(b) display a comparison between spin-integrated ARPES data and theoretical LSDA + DMFT + 1SM calculations of Fe(110) along the ΓN direction of the bulk Brillouin zone (BZ) with p polarization. The k values were calculated from the used photon energies ranging from 25 to 100 eV, using an inner potential $V = 14.5$ eV. Figure 2 displays analogous spin-resolved ARPES data for p and s-polarized photons together with LSDA + DMFT + 1SM calculations.

Near the Γ point ($k \sim 0.06\Gamma N$), the intense peak close to the Fermi level corresponds to a $\Sigma^{\downarrow}_{1,3}$ minority surface resonance. Experimentally, its $\Sigma^{\downarrow}_{3}$ bulk component crosses the Fermi level at $k \sim 0.33\Gamma N$, leading to a reversal of the measured spin polarization and to a strong reduction of the intensity at $k = 0.68\Gamma N$ in the minority channel, in agreement with the theoretical results [Figs. 2(b) and 2(d)]. The peak at the binding energy BE ~ 0.7 eV, visible mainly for p polarization in a large range of wave vectors between Γ and N, can be assigned to almost degenerate $\Sigma^{\uparrow}_{1,4}$ bulklike

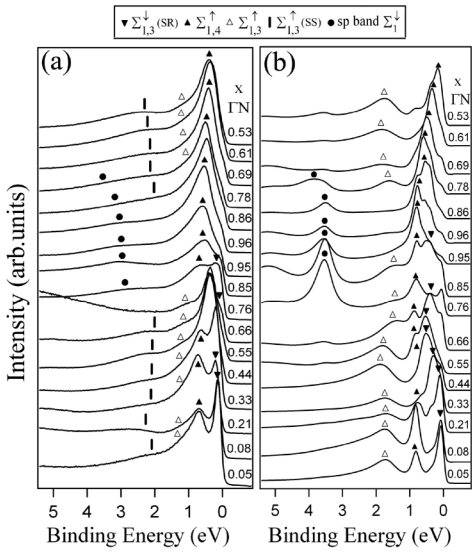

FIG. 1. (a) Experimental spin-integrated photoemission spectra of the Fe(110) surface measured with p polarization in normal emission along the ΓN direction of the bulk Brillouin zone. The curves are labeled by the wave vectors in units of $\Gamma N = 1.55$ Å^{-1}. (b) Corresponding calculations obtained by the LSDA + DMFT + 1SM method which includes correlations, matrix elements, and surface effects.

majority states [Figs. 1, 2(a), and 2(c)]. For s polarization [Figs. 2(b) and 2(d)], a $\Sigma^{\uparrow}_{3}$ feature at BE ~ 1.1 eV dominates the spectrum at the Γ point. For p polarization, its degenerate $\Sigma^{\uparrow}_{1}$ states form a shoulder around the same BE. The broad feature around 2.2 eV, visible at various k points, but not at the N point, is related to a majority $\Sigma^{\uparrow}_{1,3}$ surface state (see below). Around the N-point ($0.76 \leq k \leq 1.0$) and at BE ≥ 3 eV [Figs. 1(a) and 2(a)], we observe a $\Sigma^{\downarrow}_{1}$ band having strong sp character. The pronounced difference between its theoretical and experimental intensity distributions can be attributed to the fact that in the present calculations, only local Coulomb repulsion between d electrons is considered, without additional lifetime effects for the sp bands. When correct values for $\Im\Sigma$ for the sp-bands would be introduced, the sp features would also disappear in the calculated spectra. Finally, we notice that the background intensity of the spectrum at $k = 0.66\Gamma N$, corresponding to a photon energy of 55 eV, is strongly increasing by the appearance of the Fe $3p$ resonance.

Comparing the experimental results from spin-integrated and spin-resolved ARPES measurements with LSDA + DMFT + 1SM results, we obtain at low BE good agreement for many of the peak positions. This is also demonstrated in Figs. 3(a) and 3(b) where we compare the experimental peak positions with the LSDA + DMFT spectral function. Similar calculations based on the LSDA + 3BS scheme are compared with the experimental data in Figs. 3(c) and 3(d). Since the theoretical calculations do not show big differences, also the LSDA + 3BS spectral function agrees well at low BE with the experimental peak positions.

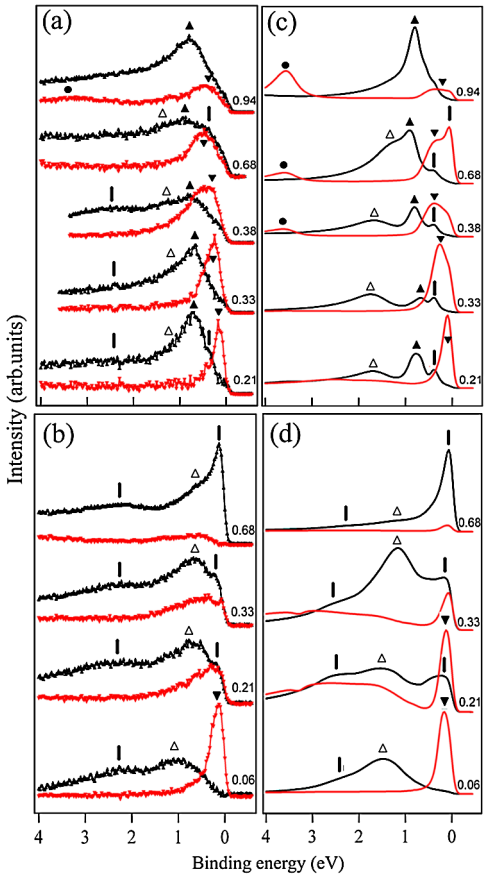

FIG. 2 (color online). Analogous data as in Figs. 1(a) and 1(b) but now spin-resolved. (a), (b) Experiment [upwards (black) triangles: majority states, downwards (red) triangles: minority states]. (c), (d) LSDA + DMFT + 1SM theory [dark (black) and light (red) lines for majority and minority electrons, respectively]. (a), (c) For *p*- and (b), (d) for *s* polarization. The symbols used for peak assignment are the same as in Fig. 1.

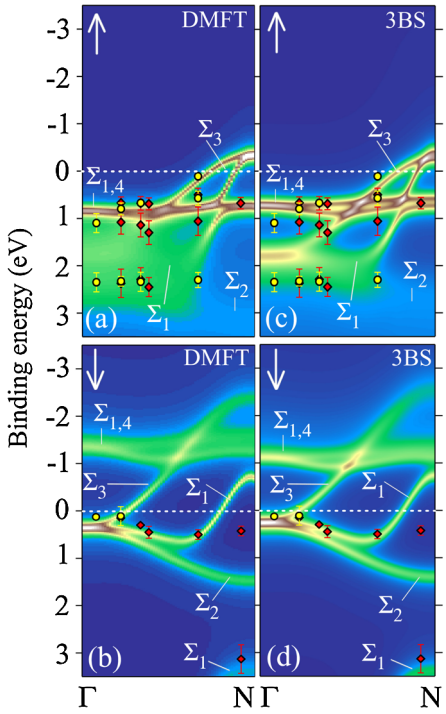

FIG. 3 (color online). Spectral functions of Fe(110) and photoemission peak positions obtained from the spin-resolved measurements for different polarizations (◇ for horizontal and ○ for vertical polarization). Results obtained by LSDA + DMFT [(a), (b)] and by LSDA + 3BS [(c), (d)] methods for majority and minority electronic states, respectively.

On the other hand, *quantitative* agreement cannot be achieved for higher BE. In particular, the calculated spectral weight near Γ for the $\Sigma^{\uparrow}_{1,3}$ bands is in between the experimental features at 1.2 and 2.2 eV. Assuming negligible correlation effects would move the calculated feature to the LDA value at BE = 2.2 eV. Thus, the experimental peak at 2.2 eV could be assigned to the bulk $\Sigma^{\uparrow}_{1,3}$ bands. However, a complete neglect of correlation effects in Fe would make the overall comparison between theory and experiment much worse. Thus, we interpret the experimental peak at BE = 2.2 eV by a $\Sigma^{\uparrow}_{1,3}$ surface state in agreement with previous experimental and theoretical studies [22]. Our theoretical results confirm this view since we clearly observe how changes in the surface barrier potential induce additional shifts in its BE position. On the other hand, we emphasize that a change in the surface barrier potential does not induce shifts in the energy position of the bulk states. Thus, from the data shown in Fig. 3, we conclude that correlation effects in the present calculations using $U = 1.5$ eV are underestimated and that a stronger band narrowing is needed to achieve agreement between theory and experiment.

Figure 4 demonstrates this for data close to the Γ point ($k = 0.05\Gamma N$). Figure 4(a) compares the experimental spin-integrated ARPES spectra with LSDA calculations broadened with the experimental energy resolution, a LSDA + DMFT calculation, and a LSDA + DMFT + 1SM calculation. At low BE, perfect agreement between theory and experiment is achieved for the minority $\Sigma^{\downarrow}_{1,3}$ surface resonance. For the bulk $\Sigma^{\uparrow}_{1,4}$ peak at BE = 0.65 eV, the agreement is less satisfactory. This holds also for the $\Sigma^{\uparrow}_{1,3}$ peak which appears in LSDA at 2.2 eV. Because of correlation effects, it is shifted in the experiment to BE ≈ 1.2 eV causing in Fig. 4(a) at that energy a shoulder and in Fig. 2(b) for $k = 0.06\Gamma N$ a peak. The difference between the ARPES data and LSDA calculations can be explained with a linear $\Re\Sigma = 0.7E$ corresponding to a mass enhancement $m^*/m_0 = 1.7$, where m_0 is the bare-particle mass. This experimental mass renormalization in the energy range BE ≤ 1.8 eV should be contrasted to $m*/m_0 \approx 1.25$ derived for $U = 1.5$ eV in the present work. One may speculate that the difference between the ARPES and the LSDA + DMFT + 1SM peak positions could be reduced by choosing a higher U (e.g., $U \approx 4$ eV). This value, however, is outside the previously mentioned range, and in addition, we still are left with the problem that the calculated width is far too small compared

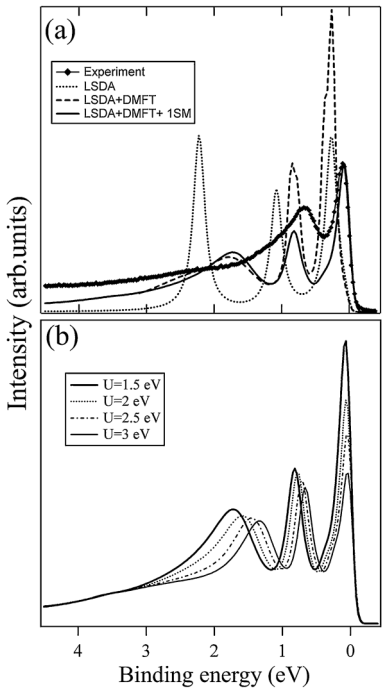

FIG. 4. (a) Comparison between the spin-integrated experimental spectra at the Γ point for p polarization with the single-particle LSDA-based calculation, the LSDA + DMFT spectra, and the LSDA + DMFT + 1SM spectra. (b) LSDA + DMFT + 1SM calculations for $U = 1.5$ to 3 eV.

with the experimental value. It is remarkable that the width does not increase with increasing U [Fig. 4(b)]. This can be explained in terms of an energy-dependent $\Im\Sigma$ and by the fact that with increasing U, the peak position moves to lower BE leading to an almost constant $\Im\Sigma$. The energy dependence of $\Im\Sigma$ also leads to slightly asymmetric peaks in the spectral function [Fig. 4(b)].

We have observed this additional broadening not only at the Γ point but also at other k values. We have fitted the spin-resolved energy distribution curves also at various k values by a sum of Lorentzians plus a background. Although we are aware that such an evaluation is problematic due to the formation of asymmetric Lorentzians discussed above, we have tried to extract $\Im\Sigma$ as a function of BE and k (not shown). From this evaluation, we obtain in a first approximation a k-independent $\Im\Sigma$, which is roughly a factor two bigger than the calculated $\Im\Sigma_{\mathrm{DMFT}}$.

We point out that this additional broadening cannot be caused by final state effects [23], since those are fully taken into account in the 1SM calculations. Furthermore, since the $3d$ bands show a rather flat dispersion, in particular, close to the high symmetry points of the BZ, the final state broadening can almost be neglected when compared with the experimental resolution. Moreover, the final state effects would cause a broadening which for a small initial state dispersion would be constant as a function of the BE. In this context, we mention that the broadening due to defect scattering is believed to be energy independent, as well.

In summary, the comparison of (spin-resolved) ARPES data of ferromagnetic bcc Fe(110) to state of the art many-body LSDA + DMFT + 1SM and LSDA + 3BS + 1SM calculations indicates that these theories lead to an important improvement compared to LSDA. However, we have demonstrated that these theories, at least in the present implementation, underestimate the mass renormalization and, in particular, the scattering rates in Fe, a typical $3d$ multiband transition metal. This result demands more refined many-body calculations, possibly with nonlocal schemes, which take into account nonlocal fluctuations in multiband systems. The long range part of the Coulomb interaction, excluded from the Hubbard model, may play a role in correcting hybridized s-p-d states. A method to overcome this limitation has been recently proposed in terms of a parameter-free extended DMFT + GW scheme [24] in which both the on-site and off-site correlations are included. Moreover the ''dual fermion'' approach [25] seems to be also promising. It would be an important step to implement this approach into realistic electronic structure calculations. These conclusions are also important for other correlated multiband systems such as Fe-pnictide high-T_c superconductors.

[1] See, e.g., C. Herring, in *Magnetism*, edited by G. T. Rado and H. Suhl (Academic Press, New York, 1966), Vol. IV.
[2] V. L. Moruzzi *et al.*, *Calculated Electronic Properties of Metals* (Pergamon Press, Oxford, 1977).
[3] For a review, see A. Georges *et al.*, Rev. Mod. Phys. **68**, 13 (1996).
[4] C. Calandra and F. Manghi, Phys. Rev. B **50**, 2061 (1994).
[5] S. Monastra *et al.*, Phys. Rev. Lett. **88**, 236402 (2002).
[6] J. Braun *et al.*, Phys. Rev. Lett. **97**, 227601 (2006).
[7] S. Hüfner, *Photoelectron Spectroscopy* (Springer Verlag, Berlin, 1995).
[8] R. O. Jones and O. Gunnarsson, Rev. Mod. Phys. **61**, 689 (1989).
[9] A. M. Turner *et al.*, Phys. Rev. B **29**, 2986 (1984).
[10] E. Kisker *et al.*, Phys. Rev. B **31**, 329 (1985).
[11] A. Santoni and F. J. Himpsel, Phys. Rev. B **43**, 1305 (1991).
[12] J. Schäfer *et al.*, Phys. Rev. Lett. **92**, 097205 (2004).
[13] J. Schäfer *et al.*, Phys. Rev. B **72**, 155115 (2005).
[14] G. C Burnett *et al.*, Rev. Sci. Instrum. **65**, 1893 (1994).
[15] J. Minár *et al.*, Phys. Rev. B **72**, 045125 (2005).
[16] J. Minár *et al.*, Phys. Rev. Lett. **95**, 166401 (2005).
[17] M. M. Steiner *et al.*, Phys. Rev. B **45**, 13272 (1992).
[18] M. Cococcioni and S. de Gironcoli, Phys. Rev. B **71**, 035105 (2005).
[19] S. Chadov *et al.*, Europhys. Lett. **82**, 37001 (2008).
[20] V. I. Anisimov and O. Gunnarson, Phys. Rev. B **43**, 7570 (1991).
[21] J. Braun, Rep. Prog. Phys. **59**, 1267 (1996).
[22] H. -J. Kim *et al.*, Surf. Sci. **478**, 193 (2001).
[23] N. V. Smith *et al.*, Phys. Rev. B **47**, 15476 (1993).
[24] S. Biermann *et al.*, Phys. Rev. Lett. **90**, 086402 (2003).
[25] A. N. Rubtsov *et al.*, Phys. Rev. B **77**, 033101 (2008).